Electrostatic Effects in the Kinetics of Coenzyme Binding to Isozymes of Alcohol Dehydrogenase from Horse Liver†

Hans Werner Adolph,*,‡ Martin Kiefer,‡ and Eila Cedergren-Zeppezauer§

Department of Biochemistry, Universität des Saarlandes, D-66041 Saarbrücken, FRG, and Department of Structural Chemistry, Arrhenius Laboratories for Natural Sciences, University of Stockholm, S-10691 Stockholm, Sweden

Received February 20, 1997; Revised Manuscript Received May 1, 1997⊗

ABSTRACT: The kinetic mechanism for the binding of NAD^+ and NADH to the EE and SS isozymes of alcohol dehydrogenase (LADH) was studied between pH 7 and pH 10 by monitoring the quenching of tryptophan fluorescence. A consistent interpretation of all data was only possible by introducing a two-step binding mechanism. The first binding step is related to docking of the adenosine part of the coenzymes and the subsequent isomerization to the binding of the nicotinamide part. At high NADH concentrations an additional slow isomerization was identified as a conformational transition of the protein. A pH dependence for NADH binding is observed which is restricted to changes in the binding kinetics of the adenosine moiety going from pH 7 to pH 10, a tendency which is similar also for NAD^+. This is attributed to pH-dependent variations in electrostatic attractions acting as a steering force of the docking process. The nicotinamide docking of NADH is equally fast for both isozymes and pH-independent over the measured range, whereas this docking equilibrium for NAD^+ is pH-dependent for EE- and SS-LADH alike and the rate of association comparable. Presumably, a Glu_{EE}-366−Lys_{SS} substitution results in a stronger binding and faster association of both oxidized and reduced cofactor to the SS isozyme. A structural proof is presented for coenzyme-competitive binding of a sulfate ion, resulting in electrostatic shielding.

Alcohol dehydrogenase (LADH)[1] of class I from horse liver is a long-chain, zinc-containing dehydrogenase [for classification see Jörnvall et al. (1987)]. Within this class three major isozymes exist: EE, ES, and SS [for nomenclature see Pietruszko et al. (1969)]. The E and S subunits of LADH differ by only 10 residues out of 374 amino acids totally (Park & Plapp, 1991; Hubatsch et al., 1992). Differences in binding of NADH to the EE and SS dimers were first described by Theorell et al. (1970), but rapid kinetic data for binding of NAD^+ to the SS isozyme is presented here for the first time.

Crystal structures of various complexes [see Table X in Eklund and Brändén (1987)] in different conformational states of the EE isozyme have been determined. These conformational states represent structural changes going from an open (Eklund et al., 1976) to a totally closed (Eklund et al., 1981) conformation via a partially closed structure (Cedergren-Zeppezauer et al., 1985). In addition, various, recently determined complexes including NAD(H), coenzyme, and substrate analogues have been presented (Al-Karadaghi et al., 1994; Ramaswamy et al., 1994; Li et al., 1994), but no crystal structure is available for any other horse liver isozyme. Partly on the basis of structural information a hypothetical mechanism has emerged including this conformational change, induced by coenzyme binding, as an essential step in the catalytic cycle (Eklund & Brändén, 1987).

LADH has two zinc binding sites per subunit, and both the catalytic and the structural zinc ion can be substituted by other transition metal ions. This circumstance has been utilized in numerous investigations, particularly to study the influence of coenzyme binding on the UV−visible spectra of active site substituted metals (Zeppezauer, 1986). A fully Cd(II)-substituted enzyme was used to study the binary LADH−NADH complex in solution using perturbed angular correlation of γ-ray (PAC) spectroscopy. Analysis of spectra clearly shows that two different, coexisting coordination geometries of the catalytic metal ion are present in a pH-independent equilibrium. One interpretation of this observation is that open and closed conformational states of the protein might influence the inner sphere coordination geometry of the active site metal ion differently (Hemmingsen et al., 1995).

Coenzyme binding to LADH and its pH dependence have been studied with different techniques using various experimental approaches [for review see Ohno and Ushio (1987)]. Measurements have often been performed under substantially different conditions, and it is therefore difficult to get a complete and consistent view of the coenzyme binding mechanism from data in the literature. A comparison of isoenzymes with respect to coenzyme binding thus required

† This work was supported by the Deutsche Forschungsgemeinschaft and the Universität des Saarlandes.

* Author to whom correspondence should be addressed: telephone, 49-681-302-2492; FAX, 49-681-302-2097; E-mail, hwadolph@rz.uni-sb.de.

‡ Universität des Saarlandes.

§ University of Stockholm.

⊗ Abstract published in *Advance ACS Abstracts,* July 1, 1997.

[1] Abbreviations: LADH, horse liver alcohol dehydrogenase (E.C. 1.1.1.1); EE-, SS-, and ES-LADH, isozymes of LADH (E for "ethanol active" and S for additionally "steroid active"); NADH, reduced nicotinamide adenine dinucleotide; NAD^+, oxidized nicotinamide adenine dinucleotide; ADPR, adenosine(5′)diphospho(5)-β-D-ribose; MPD, 2-methyl-2,4-pentanediol; DMSO, dimethyl sulfoxide; TES, 2-[[tris(hydroxymethyl)methyl]amino]ethanesulfonic acid; TAPS, 3-[[tris(hydroxymethyl)methyl]amino]propanesulfonic acid; BisTrisPropane, 2-[bis(2-hydroxyethyl)amino]-2-(hydroxymethyl)-1,3-propanediol.

S0006-2960(97)00398-X CCC: $14.00

a new determination of binding equilibria and kinetics under standardized experimental conditions.

Different electrostatic models have evolved to explain the pH dependence of coenzyme binding parameters. A zinc-bound water molecule (Theorell & McKinley-McKee, 1961; Kvassman & Pettersson, 1979; Andersson et al., 1981), Lys-228 (Kvassman & Pettersson, 1987), and His-51 (Cook & Cleland, 1981; Eftink & Byström, 1986) have been suggested as relevant pK_a groups.

Until now binding of NADH has been considered a one-step process (Geraci & Gibson, 1967) in most of the publications dealing with coenzyme binding kinetics. A two-step mechanism has been suggested for mutants of human LADH (Stone et al., 1993). From pressure relaxation studies it was concluded that an isomerization of the LADH−NAD^+ complex is rate-limiting for NAD^+ association (Coates et al., 1977). A minimum two-step mechanism was suggested as a necessary assumption to explain a limiting rate of 500 s^{-1} for NAD^+ association obtained from stopped-flow experiments (Sekhar & Plapp, 1988).

It is shown here that binding of NAD^+ as well as NADH can be described as a two-step mechanism, and data are presented from which all four rate constants involved in this process for each isozyme have been determined. Moreover, we provide evidence that the two-step mechanism applied here is still unable to explain all experimental findings. Our results support earlier observations that binding of NADH becomes more complicated at high coenzyme concentrations (Kovár & Klukanová, 1984). Under such conditions a second slow isomerization step is observed and the possible nature of this isomerization is discussed in the light of results obtained with NADH binding studies to the heterodimer ES-LADH.

MATERIALS AND METHODS

The purification of the isozymes EE, ES, and SS of LADH is described elsewhere (Hubatsch et al., 1995). The purity of isozymes was tested by SDS−PAGE and native PAGE, and both methods resulted in single protein bands. Protein concentration was determined using $\epsilon_{280} = 18200\ M^{-1}\ cm^{-1}$, a value being identical for all three isozymes. The concentrations of active enzymes were determined by active site titrations (Einarsson et al., 1976). NAD^+, free acid grade I, 100%, and NADH, disodium salt grade 1, 100%, were purchased from Boehringer/Mannheim and used without further purification. The concentrations of NADH and NAD^+ solutions were determined using $\epsilon_{340} = 6220\ M^{-1}\ cm^{-1}$ and $\epsilon_{260} = 18000\ M^{-1}\ cm^{-1}$, respectively. Buffer substances used were of highest available purity, and solutions were prepared using doubly destilled water. Buffers used were 0.1 M TES/KOH at pH 7, 0.1 M TAPS/KOH at pH 8.5, and 0.1 M BisTrisPropane/HCl at pH 10. All kinetic experiments described were performed at 25 °C.

Crystallization and X-ray Structure Analysis of an EE-LADH−Sulfate Complex. Crystals were grown in dialysis experiments at 4 °C. A 1% (w/v) enzyme solution (2 mL) in 40 mM Tris-HCl, pH 8.2, and 25 mM Na_2SO_4 was dialyzed against 15 mL of 40 mM Tris-HCl, pH 8.2, to which increased concentrations of 2-methyl-2,4-pentanediol (MPD) was added during a period of several weeks. Crystals did grow at a final concentration of 8% MPD. Subsequently PEG-400 was slowly added to a final concentration of 25%. This MPD/PEG mixture served as the cryoprotectant during flash cooling of crystals in a nitrogen stream.

Data were collected to 1.6 Å resolution, 99.1% all over completeness, at the beam line BW7B ($\lambda = 0.873$ Å) at EMBL, Outstation Hamburg. One crystal about 0.2 mm in size in all dimensions was mounted on a loop (Teng, 1990), and data were collected at 140 K. The space group is $C222_1$ with cell parameters $a = 55.28$ Å, $b = 70.87$ Å, and $c = 179.94$ Å. The structure was solved using the molecular replacement method, utilizing as a search model the coordinates of the open conformation of LADH (Eklund et al., 1976), deposited at the Brookhaven Protein Data Bank (Bernstein et al., 1977). A complete account of the refinement and a detailed description of the structure will be published elsewhere (E. Cedergren-Zeppezauer, H. W. Adolph and Z. Dauter, unpublished results).

Fluorescence Titrations. Fluorometric measurements were performed using the spectrofluorometer MPF 44A from Perkin-Elmer. The quenching of protein fluorescence was detected at 330 nm with an excitation wavelength of 285 nm. A 320 nm cutoff filter was used in the emission light path. The relative fluorescence was corrected for inner filter effects (Luisi & Favilla, 1970). For absorption measurements the spectrophotometer Lambda 9 from Perkin-Elmer was used.

Kinetic Measurements. The transient kinetic measurements were performed with the stopped-flow spectrofluorometer DX17MV from Applied Photophysics equipped with a 150 W xenon arc lamp. Protein fluorescence was measured with excitation at 285 nm and detection of emitted light using a cutoff filter which allows transmission of light >310 nm. Reactions could be followed with a dead time of 1.3 ms, allowing detection of rate constants up to 1500 s^{-1}. The enzyme concentrations after mixing were in the range of 10−1000 nM with a >10-fold excess of coenzyme. To improve the signal-to-noise ratio, 5−12 reaction traces were averaged before fitting the data. A monoexponential equation was fitted to data obtained for NAD^+, throughout. Binding of NADH resulted in monoexponential relaxations at low coenzyme concentrations whereas a sum of two monoexponential equations was used for fitting to data obtained at high NADH concentrations (see below). The k_{app} values for the faster process are shown in the figures.

The displacement reaction of ADPR with NADH was performed by mixing enzyme, preequilibrated with ADPR in a concentration resulting in >90% saturation, with varying concentrations of NADH. The saturation curves obtained from the slower phase of biexponential fits were evaluated by fitting a hyperbolic function to the data (a small fraction of enzyme was always free from ADPR). The k_{max} value obtained for infinite NADH concentration was taken as the dissociation rate constant of ADPR.

All experiments were repeated two to three times in completely independent series to verify the results obtained. Some of the plots in the figures shown below are composed of data from different experimental series. Steady-state kinetic experiments were performed as previously described (Adolph et al., 1991).

Data Analysis. For fitting of analytical equations to data, the program Sigma Plot 5.0 from Jandel Scientific was used. It allows fitting of data to arbitrary user-defined equations using a Levenberg−Marquardt algorithm. A different approach for fitting and simulation of data is realized in the

Table 1: Kinetic Rate Constants for Binding of the Coenzymes NADH and NAD^+ and the Coenzyme Fragment ADPR to EE- and SS-LADH, Equilibrium Binding Constants for NADH and NAD^+, and k_{cat} for Ethanol from Steady-State Experiments

		EE-LADH			SS-LADH		
method used	constant	pH 7	pH 8.5	pH 10	pH 7	pH 8.5	pH 10
			NADH				
	k_1 (M^{-1} s^{-1} × 10^6)	54.3	29.9	3.67	221[a]	118[a]	32.4[a]
nonlinear regression analysis	k_{-1} (s^{-1})	328[a]	388[a]	1088[a]	68[a]	99[a]	213
using eq 1	k_2 (s^{-1})	1238[a]	1391	1268	778[a]	1088[a]	913
	k_{-2} (s^{-1})	20.4	16.8	16.8	16.17	25.8	18.96
calculation from kinetic rate constants with eq 4	$K_{B,\,calc}$ (M^{-1} × 10^6)	10.2	6.48	0.259	160	52	7.48
equilibrium binding experiment	K_B (M^{-1} × 10^6)	10.7 (±2.0)	6.48 (±1.11)	0.303[b]	60.9 (±7.1)	64 (±27)	11.1[b]
linear regression analysis of the	k_{on} (M^{-1} s^{-1} × 10^6)	36.2	23.4	1.86	205	109	25.8
linear part of saturation	k_{off} (s^{-1})	2.14	4.8	6.5	(−7.7)	(−9.4)	1.43
curves (eq 2)	R	0.9980	0.9960	0.9900	0.997	0.9995	0.9990
	no. of data points	7	7	6	4	7	12
biexponential fits (see Scheme 2)	k_{-3} (s^{-1})	65 (±25)	70 (±25)	nd[c]	62 (±25)	60 (±25)	nd[c]
			NAD^+				
	k_1 (M^{-1} s^{-1} × 10^6)	55.5	8.32	1.19[a]	193[a]	55.4[a]	7.7
nonlinear regression analysis	k_{-1} (s^{-1})	1954	1169	1303	1041	186	394
using eq 1	k_2 (s^{-1})	554	685	797	469	722	963
	k_{-2} (s^{-1})	434	45.9	5.4	448	86.57	18.5
calculation from kinetic rate constants with eq 4	$K_{B,\,calc}$ (M^{-1} × 10^6)	0.065	0.113	0.134	0.38	2.75	1.04
equilibrium binding experiment	K_B (M^{-1} × 10^6)	0.078 (±0.013)	0.174 (±0.026)	0.18[d]	0.86 (±0.20)	2.83 (±0.67)	nd
linear regression analysis of the	k_{on} (M^{-1} s^{-1} × 10^6)	15.4	2.7	0.415	59.6	38.9	4.35
linear part of saturation curves	k_{off} (s^{-1})	317	32.4	4.04	289	30.0	14.43
(eq 2)	R	0.7880	0.9955	0.9999	0.9942	0.9237	0.9978
	no. of data points	6	9	6	4	4	5
			ADPR				
replacement with NADH	k_{off} (s^{-1})	328 (±12)	388 (±3)	1088 (±48)	68 (±5)	99 (±10)	232 (±10)
			Ethanol				
steady-state kinetics	k_{cat} (s^{-1})	2.9	3.99	6.55	1.05	1.24	4.8

[a] These rate constants were fixed in the final fit of eq 1 to the data. [b] Theorell et al., 1970; the buffer used was 0.1 M Tris-HCl. [c] Saturation could not be reached (see Results section). [d] Taniguchi et al., 1967; the buffer used was 0.1 M Tris-HCl.

Scheme 1

$$\text{LADH} + \text{NAD(H)} \underset{k_{-1}}{\overset{k_1}{\rightleftharpoons}} \text{LADH-NAD(H)} \underset{k_{-2}}{\overset{k_2}{\rightleftharpoons}} \text{LADH}^*\text{-NAD(H)}$$

program Chemsim. It simulates chemical reactions by numerical integration of the underlying differential equation system. It allows the simulation and analysis of kinetic and thermodynamic experiments using sets of rate equations, combined rate equations and equilibria [compare Adolph et al. (1991)], or arbitrary combinations of coupled equilibria. The Chemsim program was used to fit a single binding site scheme to the data obtained in fluorescence titrations.

RESULTS

Evaluation of Rapid Kinetic Data. The determination of association and dissociation rate constants was performed using nonlinear regression analysis of plots with observed rate constants (k) *vs* ligand concentration. For both NAD^+ and NADH the apparent association rate constants (k_{app}) saturate with increasing coenzyme concentration resulting in a limiting value (k_{max}). The minimal mechanism describing the experimental data is represented in Scheme 1 containing a rate-limiting isomerization step (k_2).

The absence of biexponential relaxations observed in the low and medium coenzyme concentration range implies that the first reaction step in Scheme 1 results in no change in fluorescence. Quenching of Trp-314 fluorescence presupposes binding of the nicotinamide ring (Strambini & Gonnelli, 1990). Thus step 2 in Scheme 1 is the only fluorescence changing step and is coupled to docking of the nicotinamide moiety of the coenzymes. Saturation of k_{app} could be alternatively explained with a two-step mechanism whose first step was an equilibrium of two enzyme states from which only one could bind coenzyme. However, this mechanism does not account for the marked differences in the binding kinetics of NAD^+ and NADH, whereas Scheme 1 does.

Equation 1 is generally valid for a two-step binding mechanism (Scheme 1) and was used for fitting the data (Hiromi, 1979). Due to the limited quality of experimental

$$k_{app} = 0.5(k_1[\text{NAD(H)}] + k_{-1} + k_2 + k_{-2}) - \{0.25(k_1[\text{NAD(H)}] + k_{-1} + k_2 + k_{-2})^2 - k_1[\text{NAD(H)}](k_2 + k_{-2}) - k_{-1}k_{-2}\}^{1/2} \quad (1)$$

data obtainable unconstrained fits of eq 1 resulted in the final rate constants in only three cases. Unconstrained fits of eq 1 to the NADH binding curves usually resulted in negative numbers for k_{-2}, which numerically contributes little to k_{app}. (The experimental errors in the single points at high NADH concentrations are of a magnitude comparable to the magnitude of k_{-2}.) The slope of the linear part of the saturation curves, however, contains no contribution of k_{-2}

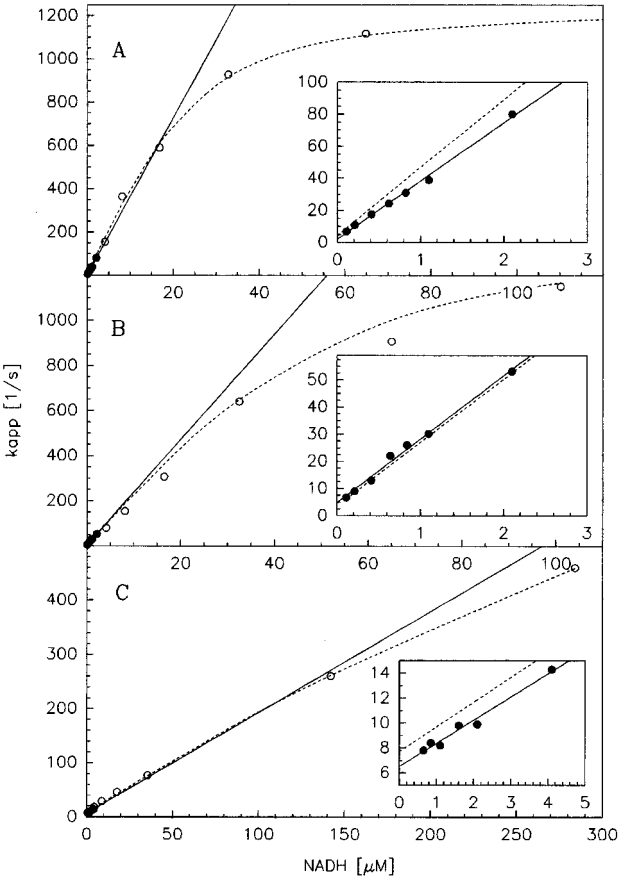

FIGURE 1: Kinetics of binding of NADH to the EE isozyme of LADH. Experimental data are shown for (A) pH 7.0, (B) pH 8.5, and (C) pH 10.0. The dashed lines represent fits of eq 1 to the complete set of data (● and ○), whereas the full lines represent a linear regression to the linear part (●) of the saturation curves. The insets are magnifications of the low concentration range. The rate constants obtained from the fits are listed in Table 1. (A) The limiting rate constant under saturating conditions obtained from an unconstrained fit of eq 1 was used to constrain the rate constant of nicotinamide docking (k_2). Additionally, it was assumed that k_{-1} equals the dissociation rate constant of ADPR under identical conditions. Thus k_{-1} and k_2 were constrained for fitting of eq 1. (B and C) k_{-1} was assumed to equal the ADPR dissociation rate constant under the corresponding conditions and constrained for fitting of eq 1. At pH 10 saturation could not be reached due to high absorbance of NADH.

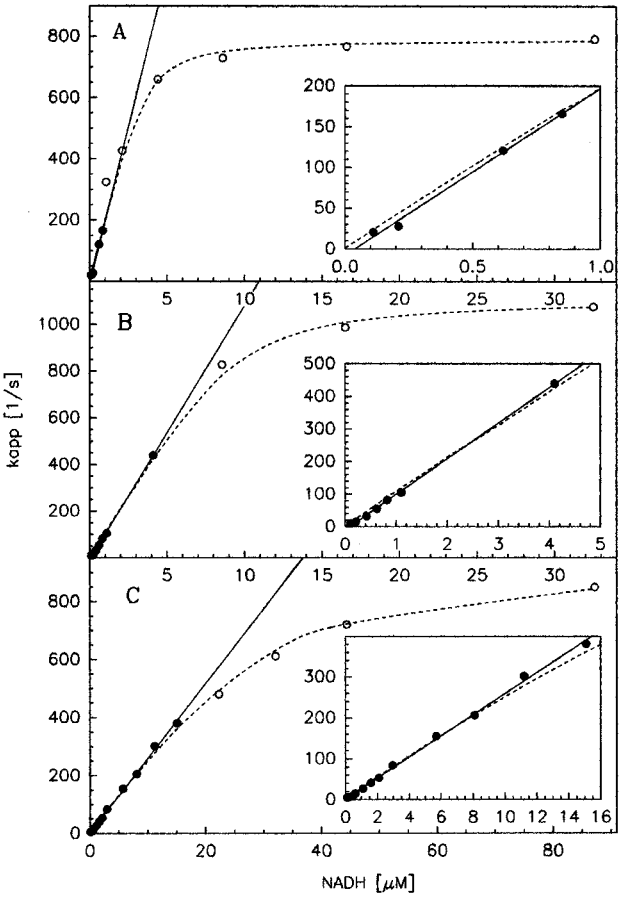

FIGURE 2: Kinetics of binding of NADH to the SS isozyme of LADH. Experimental data are shown for (A) pH 7.0, (B) pH 8.5, and (C) pH 10.0. The dashed lines represent fits of eq 1 to the complete set of data (● and ○), whereas the full lines represent a linear regression to the linear part (●) of the saturation curves. The insets are magnifications of the low concentration range. The rate constants obtained from the fits are listed in Table 1. (A and B) k_{-1} was constrained to the ADPR dissociation rate constant and k_2 was obtained from an unconstrained fit of eq 1. From the slope of the linear part of the saturation curve k_1 was calculated with k_{-1} and k_2. The dotted line represents a fit of eq 1 with k_1, k_{-1}, and k_2 constrained. (C) k_1 was obtained according to the procedure described for (A) and (B) and constrained for fitting of eq 1.

(see below). The difficulties in fitting eq 1 could be overcome by introducing constraints based on the well-founded assumptions that (i) the first half of Scheme 1 represents binding and dissociation of the adenosine moiety of the coenzyme (rate constants k_1 and k_{-1}) followed by the docking/removal process of the nicotinamide part (k_2, k_{-2}) in accordance with Kvassman and Pettersson (1987) and (ii) the dissociation rate constant of ADPR obtained from displacement reactions with NADH equals the dissociation rate constant of the adenosine moiety of NADH and could be used to constrain k_{-1}.

Far from saturation k_{app} depends linearly on the NAD(H) concentration, and apparent association (k_{on}) and dissociation rate constants (k_{off}) can be obtained from fits of eq 2 and

$$k_{app} = k_{off} + k_{on}[\mathrm{NAD(H)}] \qquad (2)$$

allow for a direct comparison with corresponding data published by others (Table 1). Depending on the relative magnitude of rate constants in Scheme 1, k_{off} and k_{on} from eq 2 are determined by a combination of rate constants. In cases with $k_{-1}/k_1 >$ [NAD(H)] and k_2 and k_{-1} being of comparable magnitude, eq 3 results for the linear part of the

$$k_{app} = k_{-2} + (k_1k_2/(k_{-1} + k_2))[\mathrm{NAD(H)}] \qquad (3)$$

saturation cuves (Fersht, 1977).

The slope in eq 3 is determined by only three of the four rate constants from Scheme 1. Thus the knowledge of two rate constants (namely, k_{-1} and k_2) could be used to calculate the third one (k_1). In case of NADH binding the dissociation rate constant of ADPR obtained from replacement kinetics with NADH was used to constrain k_{-1}. In some cases the limiting rate constant under saturating conditions (k_{max}) was additionally used to constrain k_2 (k_{-2} proved to be $<< k_2$ resulting in an error of approximately 2% in the estimated k_2). Subsequently, k_1 could be calculated from the slope of the linear part of the saturation curves according to eq 3. Depending on the respective quality of experimental data, one to 3 of the rate constants in eq 1 were constrained in the fits presented (see legends to Figures 1 and 2 for details). The quality of data obtainable for binding of NAD^+ was

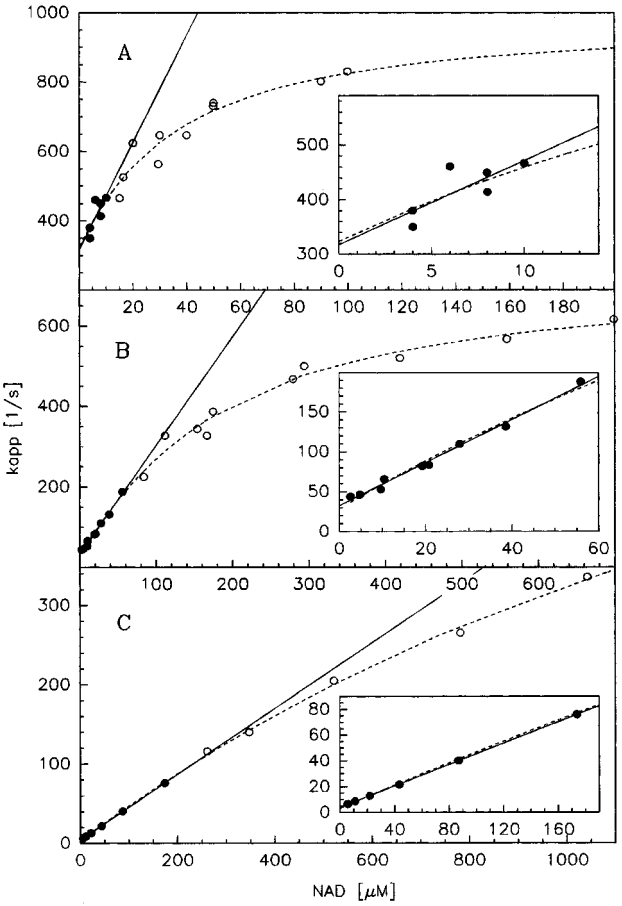

FIGURE 3: Kinetics of binding of NAD^+ to EE-LADH. Experimental data are shown for (A) pH 7.0, (B) pH 8.5, and (C) pH 10.0. The dashed lines represent fits of eq 1 to the complete set of data (● and ○), whereas the full lines represent a linear regression to the linear part (●) of the saturation curves. The insets are magnifications of the low concentration range. The rate constants obtained from the fits are listed in Table 1. (A and B) The dotted lines represent unconstrained fits of eq 1 to the data. (C) An unconstrained fit of eq 1 was used to obtain estimates for k_{-1} and k_2. These were used to calculate k_1 from the slope of the linear part of the saturation curve. The fit shown was obtained with k_1 constrained to the calculated value. At pH 10 saturation could not be reached due to high light absorbance of NAD^+.

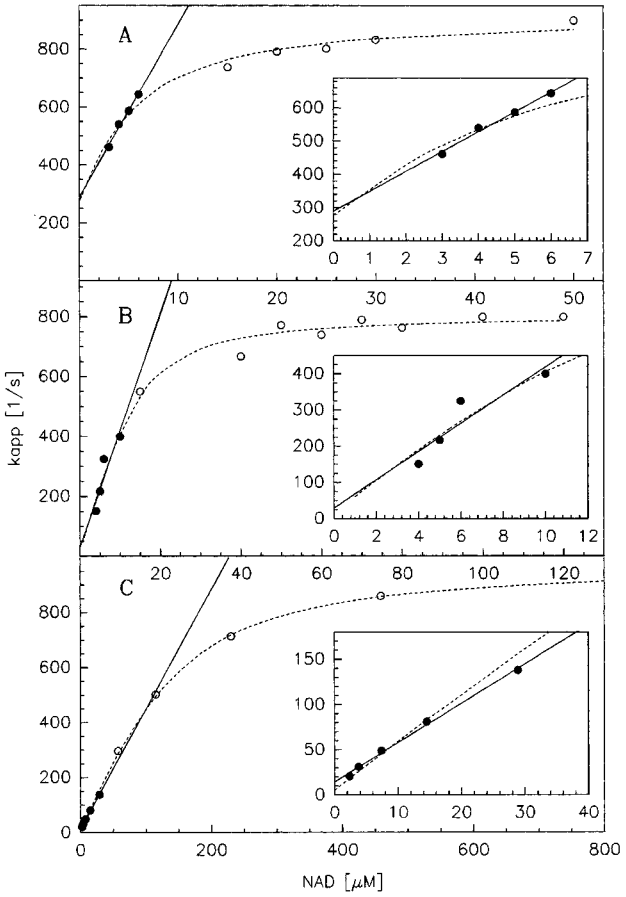

FIGURE 4: Kinetics of binding of NAD^+ to SS-LADH. Experimental data are shown for (A) pH 7.0, (B) pH 8.5, and (C) pH 10.0. The dashed lines represent fits of eq 1 to the complete set of data (● and ○), whereas the full lines represent a linear regression to the linear part (●) of the saturation curves. The insets are magnifications of the low concentration range. The rate constants obtained from the fits are listed in Table 1. (A and B) Fitting was performed as described for Figure 3C. (C) Unconstrained fit of eq 1 to the data.

poor in some cases due to the small variation of k_{app} values over the measurable coenzyme concentration range (SS-LADH at pH 7.0 and 8.5) combined with a high error level or due to the fact that saturation could not be reached (EE-LADH at pH 10) (see Figures 3 and 4). An approximative way of fitting the data was used. Unconstrained fits of eq 1 resulted in estimates for k_{-1} and k_2. These were used to calculate k_1 from the slope of the linear part of the saturation curves. Finally, the calculated k_1 was constrained in the fit of eq 1. This procedure results in weighting of the data in favor of the low concentration range. Whereas k_1 and k_{-2} show clear tendencies upon pH variation, the numerical values obtained for k_{-1} and k_2 are considerably less reliable as compared to the corresponding data obtained for NADH binding.

The reliability of the rate constants finally obtained was tested by comparison of the overall equilibrium binding constant calculated according to the minimal mechanism (Scheme 1) (eq 4) with the corresponding experimentally determined binding constants.

$$K_B = k_1(k_2 + k_{-2})/k_{-1}k_{-2} \quad (4)$$

Rate Constants and Equilibrium Binding Constants for NAD$^+$, NADH, and ADPR. Figures 1−4 summarize the kinetic experiments for binding of NAD^+ and NADH to EE- and SS-LADH. Each figure contains three sets of data: measurements at pH 7, pH 8.5, and pH 10. (The insets in the figures represent magnifications of the low concentration range of the saturation curves together with the corresponding fits.)

Saturation of apparent first-order rate constants occurs at high concentrations of NAD^+ and NADH. Consequently, binding can be explained by a two-step mechanism according to Scheme 1.

For the pH values investigated and for both isozymes a limiting rate for the association of NADH is observed. Independent of pH a fit of eq 1 results in an average value for $k_{2,NADH} = 1300\ (\pm 66)\ s^{-1}$, corresponding to nicotinamide binding to EE-LADH. For the SS isozyme this value is $k_{2,NADH} = 926\ (\pm 127)\ s^{-1}$ and also independent of pH. The rate constant $k_{-2,NADH}$ is independent of pH and of the same magnitude for both isozymes within experimental error [18 ± 1.7 s^{-1} (EE), 20.3 ± 4 s^{-1} (SS)]. Only $k_{1,NADH}$ and

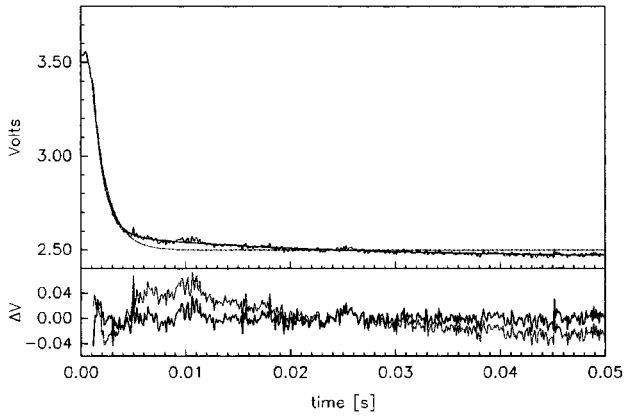

FIGURE 5: Kinetics of formation of the EE-LADH−NADH complex. The reaction was monitored as a decrease in fluorescence of LADH. $\lambda_{ex} = 285$ nm, $\lambda_{em} > 310$ nm, [EE-LADH] = 0.8 mM, [NADH] = 32 mM, 0.1 M TES/KOH, pH 7.0, 25 °C. The data shown are the average of five reaction traces. Only data obtained >1.75 ms after mixing were used for fitting. Two alternative fits are shown. The dashed line represents the fit of a single exponential function resulting in $k_{app} = 698$ s^{-1} with an amplitude of $\Delta V = 1.87$ V. The full line is a fit of a double exponential equation resulting in $k_{app,1} = 973$ s^{-1} ($\Delta V = 2.51$ V) and $k_{app,2} = 47.8$ s^{-1} ($\Delta V = 0.13$ V).

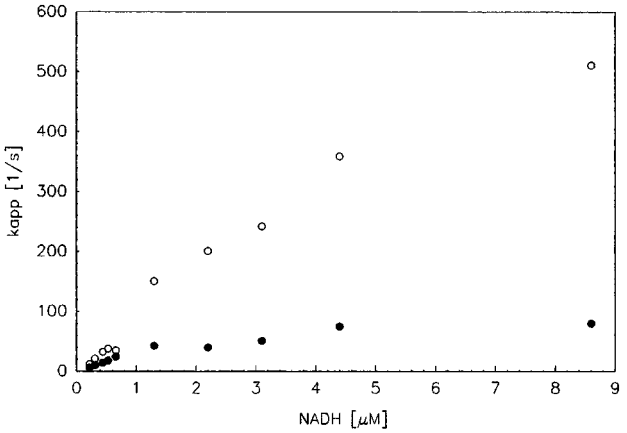

FIGURE 6: Kinetics of binding of NADH to ES-LADH in 0.1 M TAPS/KOH, pH 8.5. The data shown represent the k_{app} values obtained from fits of a two-exponential equation to the data (○ for the fast relaxation corresponding to the S subunit and ● for the slow relaxation corresponding to the E subunit). For the slow relaxation a limiting rate of 80 s^{-1} is observed, whereas the fast relaxation shows data comparable to the SS isozyme.

$k_{-1,NADH}$, association and dissociation of the adenosine part, show significant effects of the pH variation between 7 and 10. The second-order rate constant for the association process ($k_{1,NADH}$) of both isozymes strongly decreases upon increasing pH whereas $k_{-1,NADH}$ increases by a factor of 3. $k_{1,NADH}$ is faster for the SS isozyme and $k_{-1,NADH}$ is substantially decreased. Equilibrium binding constants calculated with eq 4 are in good agreement with experimentally determined values (Table 1). $k_{off,NADH}$ obtained from linear regression to the low concentration range for the EE isozyme is in good agreement with k_{cat} values obtained from steady-state kinetics with ethanol (Table 1). For ADPR k_{off} is pH-dependent for both isozymes, increasing by a factor of 3 between pH 7 and pH 10. At each pH $k_{off,ADPR}$ is slower by a factor 4−5 in case of SS- as compared to EE-LADH.

Extension of the NADH Binding Mechanism. At high concentrations of NADH subsequently to the first relaxation step a second slow relaxation was observed at pH 7 and pH 8.5, indicating an additional reaction step compared to NAD^+. This process, which cannot be explained with Scheme 1, results in a further decrease of the protein fluorescence (Figure 5) and the rate constants obtained are independent of the coenzyme concentration and identical at pH 7 and pH 8.5. At pH 10 this reaction was not observed, which could be due to the high NADH concentrations needed to reach saturating conditions (see Figure 1C for the EE isozyme). The data given for k_{-3} in Table 1 are averages of the results from biexponential fits to reaction traces obtained with various saturating concentrations of NADH. A mechanistic interpretation in terms of an additional isomerization step is facilitated if experimental data obtained with the heterodimeric ES isozyme are compared to the corresponding results with the homodimers. Figure 6 shows the binding kinetics of NADH to the ES isozyme at pH 8.5. In the low concentration range the slope of the saturation curves is similar to the data obtained for EE- and SS-LADH. With increasing NADH concentration the fast relaxation, corresponding to the S subunit, saturates comparable to the SS isozyme. But differently to the EE isozyme the slow phase, corresponding to the E subunit, shows a limiting rate of approximately 80 s^{-1}. Since Scheme 1 is not able to explain the NADH binding kinetics at high coenzyme concentrations, the coenzyme binding mechanism was extended to include an additional conformational change of the protein (Scheme 2). Scheme 2A shows the binding of NADH to the homodimers. E* (EE or SS isozyme) denotes a complex showing quenching of protein fluorescence. Two conformations of the protein are introduced (o, for "open conformation"; c, for "closed conformation"). The slow isomerization observed is related to the transition between E^*_o and E^*_c with one NADH bound to the dimer (k_{-3}). In the case of the ES isozyme Scheme 2B has to be considered. Since k_{1S} equals 4 times k_{1E}, the S subunit binds the first NADH molecule with high probability, resulting in an equilibrium of open and closed conformations of both subunits. Under the assumption that LADH in the closed conformation is unable to bind NADH, k_{-3S} equals the limiting association rate constant for the E subunit of ES-LADH.

Sulfate Ion as a Coenzyme-Competitive Inhibitor. In an X-ray investigation of the coenzyme-free EE isozyme made on crystals grown from a solution containing 1 mM sodium sulfate, the binding of one sulfate ion per subunit could be observed. Sulfate occupies the pyrophosphate binding site in the coenzyme binding crevice bridging Arg-47 and Arg-369 (Figure 7). Both residues are involved in the neutralization of the pyrophosphate group in NAD(H)-containing structures (Figure 7), but the side-chain position of Arg-47 is poorly defined in structures without an ion bound to this site (Eklund et al., 1976). Anion binding observed in the crystal at such low concentration of salt prompted a reinvestigation of the effect of sulfate ion on coenzyme binding in the concentration range corresponding to the crystallization conditions. NADH binding is indeed inhibited at very low concentrations of salt (Figure 8).

The saturation curve obtained at pH 8.5 could not be satisfactory fitted with eq 5 used earlier (Oldén & Pettersson, 1982).

$$k_{app,sulfate} = k_{app}/(1 + [SO_4^{2-}]/K_D(SO_4^{2-})) \qquad (5)$$

An alternative fit of eq 6 to the data gives a better approximation. k_{app} is the pseudo-first-order rate constant

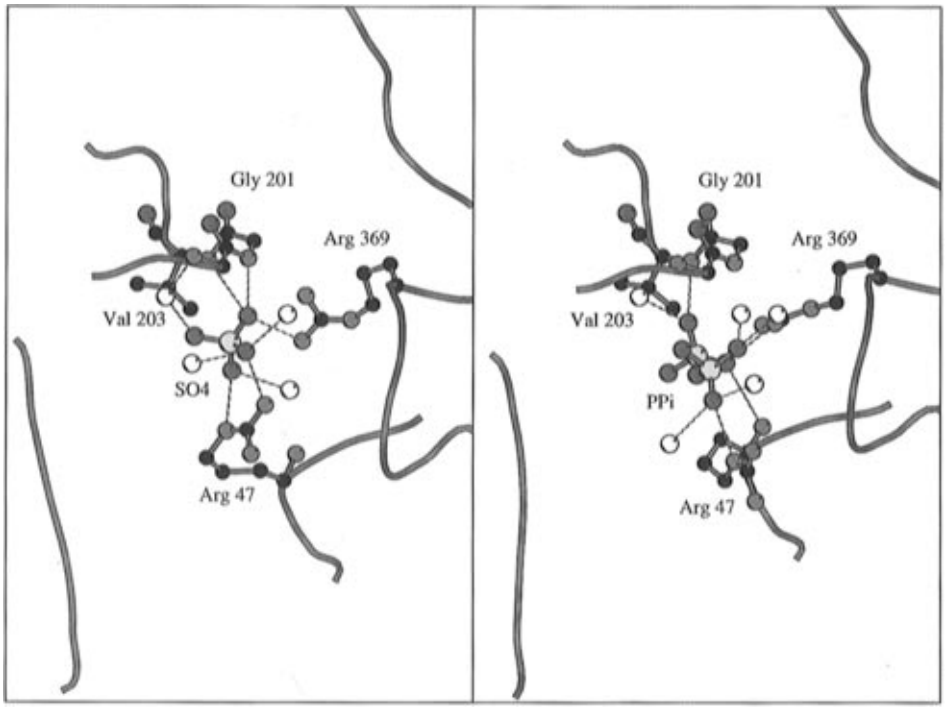

FIGURE 7: Comparison of (A, left) the binding of sulfate (SO_4) and (B, right) the binding of the pyrophosphate group of NADH (PP_i) to LADH. Interactions with solvent (white spheres) and protein main-chain and side-chain groups are shown. Data are from the structure of coenzyme-free LADH with sulfate bound to the pyrophosphate binding site (E. Cedergren, H. W. Adolph, and Z. Dauter, unpublished results) and the LADH−NADH−DMSO complex (Al-Karadaghi et al., 1994; PDB file 2OHX), respectively. The figure was generated with MOLSCRIPT (Kraulis, 1991).

Scheme 2

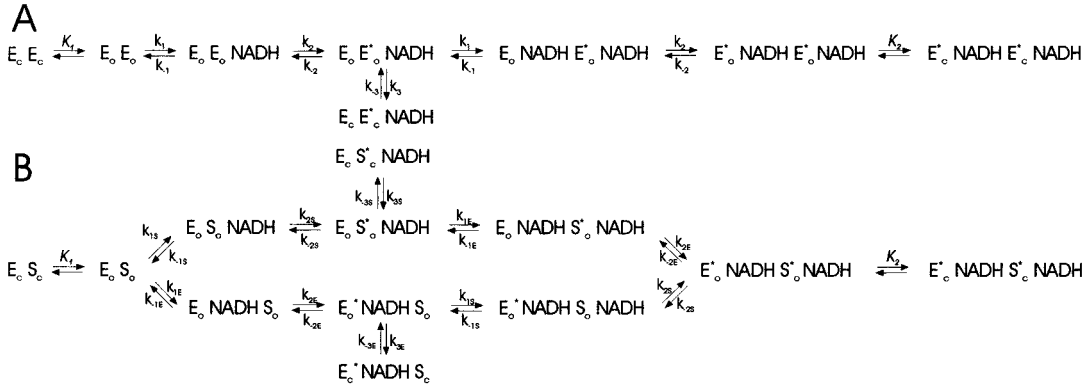

$$k_{app,sulfate} = (k_{app} - k_I)/(1 + [SO_4^{2-}]/K_D(SO_4^{2-})) + k_I \quad (6)$$

at a fixed NADH concentration without sulfate, K_D is the equilibrium dissociation constant of sulfate, and k_I in eq 6 is a limiting apparent rate constant obtained under saturating conditions of sulfate. Both fits are compared in Figure 8. Sulfate is not able to prevent NADH binding completely in the concentration range investigated but reduces k_{app} by 80% of the value measured in its absence.

Effects of pH on Single Steps of the Coenzyme Binding Mechanism. Although only three different pH values have been chosen for comparison, the data obtained were used to calculate various pK_a values for single steps of the binding mechanism of both isozymes using eq 7. In this equation

$$k_1 = (k_{1,low} - k_{1,high})/(1 + K_{app}/[H^+]) + k_{1,high} \quad (7)$$

$k_{1,low}$ stands for the limiting value for the constant k_1, adenosine docking at low pH, and $k_{1,high}$ is the limiting rate constant at high pH for the same process. K_{app} is the apparent dissociation constant for the protein group(s) participating in protonation/deprotonation reactions. Data are summarized in Table 2. pK_a values obtained for EE- and SS-LADH are very similar. The nicotinamide binding of the LADH−NAD^+ complex is influenced by pH in two ways: (1) For binding (k_2) a pK_a value around 8.4 is observed; (2) for the dissociation step (k_{-2}) a lower pK_a value (7.4−7.7) is found. The pK_a values influencing the rate constant k_1 differ for reduced and oxidized coenzyme (lowest pK_a for NAD^+ binding). This difference is most pronounced for the SS isozyme. These results indicate that the protonation state of the protein influences the association kinetics differently depending on the oxidation state of the coenzyme.

DISCUSSION

The kinetic mechanism for binding of NAD^+ and NADH to LADH shown in this work is based on a reinvestigation allowing direct comparison of all kinetic and thermodynamic parameters. The work covers the isozymes EE, ES, and SS

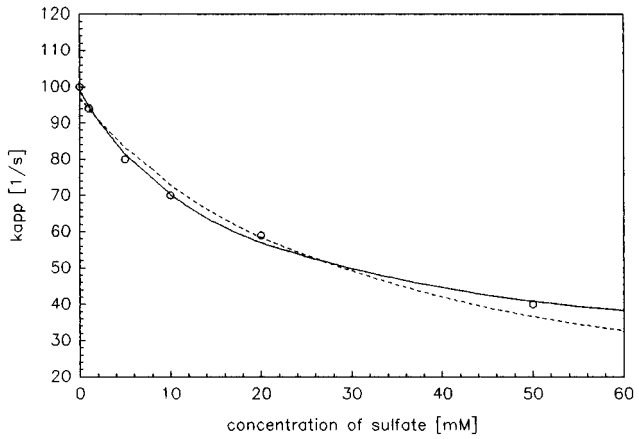

FIGURE 8: Effect of sulfate on the apparent association rate constant (k_{app}) for NADH binding to EE-LADH. The experiment was carried out at pH 8.5 with a NADH concentration of 4 mM. A fit of eq 5 to the data resulted in $k_{app} = 96.9$ (±2.2) s^{-1} and $K_D = 30.4$ (±3.3) mM (dashed line). The alternative fit of eq 6 resulted in $k_{app} = 98.9$ (±1.3) s^{-1}, $K_D = 17.3$ (±2.7) mM, and $k_I = 20.8$ (±4.5) s^{-1}.

Table 2: pH Dependence of Individual Rate Constants from Scheme 1 for Coenzyme Binding to LADH Isozymes[a]

	EE-LADH		SS-LADH	
	NAD^+	NADH	NAD^+	NADH
pK_a (k_1)	7.6	8.5	8.0	8.4
$k_{1,high\ pH}$ ($M^{-1}\ s^{-1} \times 10^6$)	0.93	1.8	5.6	27
$k_{1,low\ pH}$ ($M^{-1}\ s^{-1} \times 10^6$)	69.8	55.8	212	229
pK_a (k_2)	8.4	pH independent	8.5	pH independent
$k_{2,high\ pH}$ (s^{-1})	803		978	
$k_{2,low\ pH}$ (s^{-1})	545		452	
pK_a (k_{-2})	7.4	pH independent	7.7	pH independent
$k_{-2,high\ pH}$ (s^{-1})	4.0		16.0	
$k_{-2,low\ pH}$ (s^{-1})	620		534	

[a] Data have been obtained from fits of eq 7 or $k_{app} = (k_{low\ pH} - k_{high\ pH})/(1 + [H^+]/K_{app}) + k_{high\ pH}$ (eq 8) to data from Table 1.

of LADH and provides a new set of constants for both the oxidized and reduced cofactor over the pH range 7−10.

A consistent interpretation of all new data was only possible after a two-step binding mechanism for NAD^+ and NADH was introduced. At high NADH concentrations the mechanism was further extended, taking subunit−subunit interactions into account. We are now able to describe which individual reaction steps are responsible for differences between isozymes with reference to their pH dependences of coenzyme binding. To our opinion, no definite and fully complete description of the coenzyme binding process has been presented, in spite of the wealth of data already published.

Reasons Why the New Set of Constants Differs from Earlier Published Results. The new values for constants listed in Tables 1 and 2 significantly differ compared with literature data. This is apparently due to great differences in ionic conditions, the experimental approach, and the mechanistic models used over the past 30 years. The choice of buffer system was also found to be essential in this work (data not shown). An improved performance of today's equipment is another important factor. The association rate constants reported here exceed earlier published data by factors of 3−20 under all conditions. Individual rate constants of a two-step mechanism for NADH binding to the LADH isozymes obtained from stopped-flow experiments are reported here for the first time.

Most earlier studies were performed in phosphate buffers which were shown to be coenzyme-competitive at low pH (Oldén & Pettersson, 1982). In this investigation the presence of any significant concentration of anions, able to interfere with the coenzyme binding process, was strictly avoided. Due to longer dead times and lower sensitivity of the stopped-flow equipment available it was difficult earlier to maintain a sufficiently high excess of NADH in kinetic experiments to allow evaluation of data using the pseudo-first-order approach [e.g., Lively et al. (1987) and Theorell et al. (1970)].

At high concentrations of NADH the binding kinetics is no longer pseudo first order. Lively et al. (1987) have published data on NADH binding and fitted a monoexponential equation to progress curves which are very similar to the one shown in Figure 5 in this work, but for which only a biexponential fit is statistically valid. If the slow isomerization is ignored, underestimations of k_{app} result that are even larger in case of an increased dead time of the instrument used.

Frequently, the formation of ternary complexes was used to monitor the binding process of coenzymes. Sekhar and Plapp (1988) describe NAD^+ binding as a two-step mechanism involving a rate-limiting isomerization of the LADH−NAD^+ complex. These authors used the spectral changes occurring upon formation of the LADH−NAD^+−pyrazole ternary complex to detect binding of NAD^+. The most significant deviation from our data concerns the pH dependence of the nicotinamide docking step (k_2). Whereas Sekhar and Plapp (1988) report that k_2 depended on a group with a pK_a of 7.6 and decreases from 2500 s^{-1} (low pH) to 25 s^{-1} (high pH), we observe the opposite trend (Table 2). For both isozymes a pK_a of 8.4 and 8.5 is found, and the rate constant k_2 is higher at pH 10. Using the ternary complex formation method, the limiting rate constant detected might be the one for the association of pyrazole to the LADH−NAD^+ complex at high pH. The pK_a value (7.6) reported by Sekhar and Plapp (1988) is comparable with that found in this work (7.4) for k_{-2} of EE-LADH, associated to the dissociation step of the nicotinamide moiety.

Electrostatic Field Effects as a Steering Force of Coenzyme Binding. General Considerations. It is plaussible to assume that electrostatic forces exert an influence on the association/dissociation process of coenzyme binding to LADH since effects of pH and the presence of ions on the magnitude of rate constants are observed. Attempts have been made to identify single groups on the protein responsible for these effects [reviewed by Pettersson (1987)]. In spite of a long lasting discussion on the issue no definite experimental proof has been presented which could unambiguously sort out which of His-51 or zinc-bound water in the active site or Lys-228 (remote from the active site) is the relevant candidate. On the contrary, Lively et al. (1987) argue that none of these three electrostatic models most favored in the literature could fit their experimental data and electrostatic calculations. They conclude that the major effect of pH at low ionic strength originates from attraction/repulsion of the negatively charged coenzyme and the protein, the protein altering its overall charge from positive to negative values over the pH scale. In this investigation the ionic strength is about 0.1 M, throughout. That is within

a range where the attraction/repulsion forces are irrelevant according to Lively et al. (1987). Still, data presented here strongly indicate that electrostatic attraction/repulsion does control the coenzyme docking process.

The data presented here do not allow for a final explanation for e.g., the pH dependence of k_1. The diffusion-controlled limit for the association of a molecule like NADH is about 1−2 orders of magnitude higher as compared to the fastest second-order rate constants observed for k_1. However, the calculation of the diffusion-controlled rate constant presupposes that each encounter of an enzyme and a coenzyme molecule results in complex formation. Taking into account that the target area on the enzyme is small compared to the total surface and that a defined orientation is necessary to allow for complex formation, the calculated diffusion controlled rate constant decreases by several orders of magnitude [compare Northrup and Erickson (1992)]. We conclude that the rate constants observed at pH 7 (e.g., $k_1 = 2.2 \times 10^8$ M^{-1} s^{-1} for NADH binding to SS-LADH) are significantly higher as compared to the diffusion-controlled limit when accounting for the sterical limitations for a complex-forming encounter. Only additional steering forces are able to explain the high rate constants actually observed.

The "diffusive entrapment effect" due to Brownian motion (Northrup & Erickson, 1992) implies that during one encounter two molecules remain trapped in the vicinity of each other over a period long enough to undergo multiple collisions. During this time interval electrostatic forces can significantly influence the rate constants obtained for the association processes. If this diffusive entrapment effect is acting during coenzyme binding to LADH, the charge distribution of the protein and its changes with pH become relevant. For NADH binding only the association/dissociation of the adenosine part (k_1/k_{-1}) are influenced by pH ($pK_a = 8.5$) whereas binding of the second half of the NADH molecule into the active site, >15 Å away, is pH-independent. Possible contributions to the pK_a of 8.5 may result from the pK_a of metal-bound water reported to be 9.2, 7.6, and 11.2 for free enzyme, the enzyme−NAD^+ complex (Kvassman & Pettersson, 1979), and the enzyme−NADH complex (Andersson et al., 1981), respectively. Whereas docking of the nicotinamide ring of NAD^+ is faster at high pH (reflecting a possible attraction of the positively charged nicotinamide ring by a zinc-bound hydroxide ion), the docking of the nicotinamide ring of NADH is pH-independent [the limiting rate constant for the nicotinamide docking step (k_2) observed may result from a rate-limiting release of the numerous structured water molecules found in the active site of the coenzyme-free enzyme but not in the NADH complex]. Additional contributions to the pK_a of 8.5 could result from partial deprotonations of side chains which easily sum up to considerable changes of the net charge of the protein. The I_P of EE-LADH is close to 8.5 wheras no amino acids except Cys are reported to have such a pK_a. Possible candidates like Cys and Tyr might contribute to the overall charge density of the coenzyme binding area. Only a detailed analysis of the electrostatics of the whole molecule might be able to give a final explanation of the effects observed. We assume it to be unlikely that a single group in the active site could exclusively contribute to the pH dependence of NADH binding. We suggest that rather the net charge of the whole protein steers the process with special attractive potential for negative charges centered at the pyrophosphate binding area (Figure 9). The dipole moments of two helices (201−215 and 46−55) increase the electrostatic attracting strength of this anion binding site (Hol et al., 1978; Eklund & Brändén, 1987).

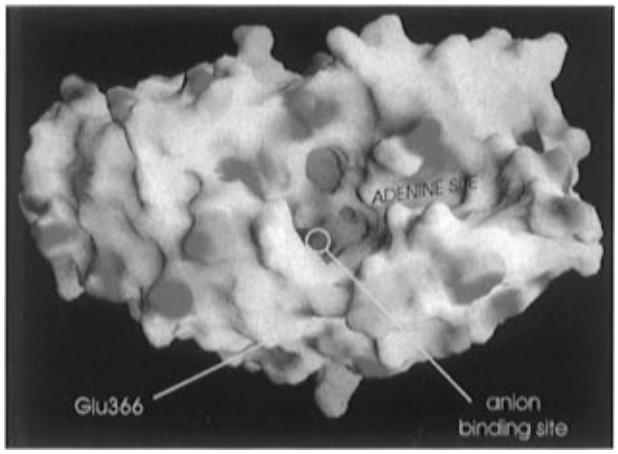

FIGURE 9: Surface representation of the EE subunit showing the charge distribution [program GRASP by Nicholls et al. (1991)]. Positively charged areas are represented in blue and negatively charged areas in red. Sulfate has been omitted from the model (anion binding site). The orientation of this view is close to the orientation of the space-filling model in Figure 10. The region corresponding to the amino acid exchange Glu_{EE}-366−Lys_{SS} is labeled.

The Effect of the Charge Differences between EE- and SS-LADH. The coenzyme binding sites in dimeric LADH are lined by a number of charged residues, and their distribution is shown in Figure 10. The total charge of the EE isozyme is positive at pH 7, neutral at pH 8.5 (I_P =8.15; Hubatsch et al., 1995), and negative at pH 10. In contrast, the SS isozyme (I_P > 10) is positively charged over the full pH range used in this work. Four out of ten amino acid exchanges in SS-LADH result in a charge shift compared to EE-LADH: Arg_{EE}-101−Ser_{SS} and Asp_{EE}-115 deleted are in close proximity to each other but located remote from the coenzyme binding site and result in no net charge difference; Glu_{EE}-17−Gln_{SS} and Glu_{EE}-366−Lys_{SS} giving a net charge difference of +6 charges/LADH molecule are in close proximity to the coenzyme binding sites (Figure 10). Experimental observations in this work directly connected to the charge differences between isozymes are summarized below: (i) Docking of the adenosine moiety, k_1, to SS-LADH is about 4 times faster than docking to the EE isozyme for NAD^+/NADH at pH 7.0 and 8.5 (corresponding to a +6 charge shift/SS-LADH molecule). (ii) $k_{off,ADPR}$(EE-LADH) is about 4 × $k_{off,ADPR}$(SS-LADH) over the pH range 7−10. (iii) Removal of the adenosine moiety, k_{-1}, from EE-LADH is about four times faster than k_{-1}(SS-LADH) for NADH over the pH range. Experimental observations with a recombinant SS-LADH with Lys-366 substituted for Glu show qualitatively similar effects (Park & Plapp, 1992): (i) $k_{cat,ethanol}$(SS-LADH mutant Lys-366−Glu) is three times faster than $k_{cat,ethanol}$(SS-LADH, recombinant wild type) and (ii) the same mutation results in a 2-fold increase of K_m(NADH).

When calculating the surface charge distribution of EE-LADH and examining the adenosine binding subsite (Figure 9), a negatively charged area emerges in the region around Glu-366. The exchange for a lysine residue in SS-LADH necessarily influences the charge at that site. Apparently, this mutation has a major influence on the binding step for

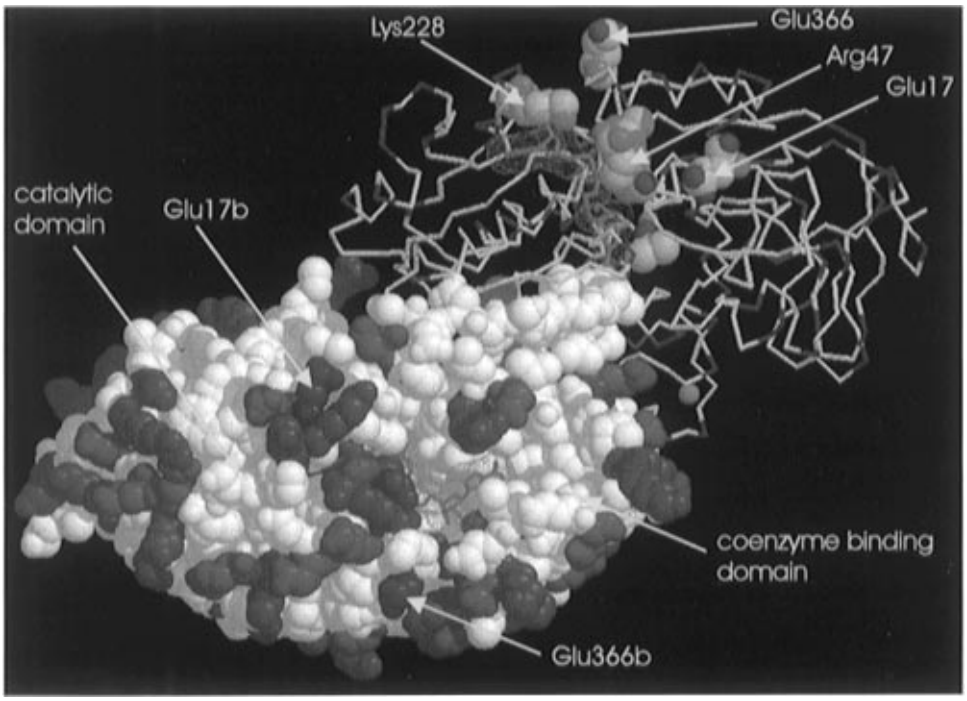

FIGURE 10: Representation of NADH binding to the EE-LADH dimer [coordinates of the LADH−NADH−DMSO complex (Al-Karadaghi et al., 1994) were used]. One subunit is represented as a space-filling model with Lys and Arg residues in blue and Glu and Asp residues in red. The NADH molecules are represented as stick models with a dotted van der Waals surface. The green space-filling residues in the center of the molecule are the Trp-314 side chains of both subunits responsible for protein fluorescence quenching. The second subunit is represented as a backbone trace with essential residues for coenzyme binding shown as space-filling models. Zn ions are represented as pink spheres. The substrate analogue DMSO is shown as a space-filling model coordinating to the active site zinc ion. The orientation of the space-filling subunit is similar to the orientation of the subunit in Figure 9 [program RasMol by Sayle (1994)].

the adenosine part of the cofactor and thus constitutes a fundamental difference between the isozymes with respect to coenzyme binding. The mutation Glu_{EE}-17−Gln_{SS}, also close to the coenzyme binding sites (Figure 10), results in the disappearance of an additional negative charge.

Sulfate Inhibition. In the X-ray structure described one sulfate ion is observed bound to the subunit of the open conformation of the EE isozyme and located at the pyrophosphate subsite of the coenzyme binding cleft. The charge of that narrow site is positive in the unliganded enzyme model as illustrated in Figure 9. Sulfate interaction with LADH is strong (K_D = 17 mM) and mimicks the pyrophosphate binding of NADH (Figure 7). The contacts to the protein involve hydrogen bonds to main-chain amide nitrogens and several water molecules in addition to Coulombic interactions (Arg-47 and Arg-369). The effect of sulfate ion on the coenzyme binding kinetics is best described by eq 6, and the inhibition can be fully understood in structural terms. An occupied site compensates 2 positive charges because the sulfate ion bridges a gap between the guanidinium groups of residues 47 (on the surface) and 369 (interior). Comparable to protonation/deprotonation reactions, interactions with an ion like sulfate are several orders of magnitude faster as compared to the binding rate constants of coenzymes [for a recent discussion of counterion effects see Mohanty et al. (1996) and references therein]. The coenzyme molecules can only "feel" the average charge of the protein at a certain pH value and a certain occupancy with, e.g., sulfate. Full occupancy with sulfate results in a NADH association rate slowed down by 80% caused by reduction of electrostatic attraction. Four positive charges per molecule are shielded, normally having an accelerating influence on binding. Thus, a difference of 4−6 unit charges per enzyme molecule correlates to a change in rate constants by a factor of 4−5. This corresponds to an incremental change of the free energies of activation of approximately 1 kJ/mol unit charge difference.

Influence of pH Variations. Opposite trends are found in the pH-dependent variation of the association and dissociation rate constant for the adenosine moiety of NADH; adenosine docking is faster at high pH but coenzyme leaves the site at a slower rate at pH 10 compared to neutral pH. Considering the diffusive entrapment effect, association and dissociation cannot be regarded as completely independent processes. During the time interval where the noncovalent bonds of the coenzyme with the protein are already broken but the coenzyme is still within the encounter distance, a high positive net charge will facilitate the reassociation process. Going from pH 10 to pH 7 results in an increase of the positive net charge of the protein accompanied by a deceleration of the adenosine dissociation (k_{-1}). In this model the increased positive potential of the coenzyme binding area for SS- as compared to EE-LADH accounts for the decelerated adenosine dissociation for NAD^+ and NADH at all pH values investigated. From a comparison of the binding kinetics of NADH and NAD^+ at fixed conditions (one isozyme at fixed pH) it becomes apparent that the adenosine dissociation is faster for NAD^+ throughout, probably due to electrostatic repulsion of the positively charged nicotinamide ring.

The nicotinamide dissociation rate constant for NAD^+, k_{-2}, depends on a group with a pK_a of 7.4, similar to what has been reported by others (Pettersson, 1987). This group has been assigned to be active site, zinc-bound water which upon NAD^+ binding dissociates to form OH^- (Theorell & McKinley-McKee, 1961). The slow release of the positively

charged nicotinamide ring from both isozymes at high pH could be explained from the presence of OH^- as the metal ligand (k_{-2} for EE-LADH is about 2 orders of magnitude different between pH 7 and pH 10, Table I). This conclusion is further supported by results recently obtained from PAC spectroscopic investigations made on the Cd-LADH−NAD^+ binary complex over the pH range 7−11 (Hemmingsen et al., 1995). Spectra could be distinguished representing a low pH and a high pH form. The interpretation is that the metal geometry at high pH having a negatively charged ligand is different from the geometry at low pH.

The Role of Conformational Transitions in the Coenzyme Binding Mechanism. For NAD^+ and NADH the association rate constants saturate with increasing coenzyme concentration, resulting in a limiting rate constant (k_{max}) which is pH-independent for NADH but not for NAD^+. The first binding step in Scheme 1 is the docking of the adenosine part of the coenzyme and gives no observable signal change in our experimental approach, whereas the docking of the nicotinamide ring (step 2 in Scheme 1) results in quenching of Trp-314 fluorescence [compare Strambini and Gonelli (1990)]. Scheme 1 does not necessarily involve a protein conformational change. In the case of NADH binding an additional slow isomerization is observed at high coenzyme concentrations.

From crystallographic investigations it has been concluded that coenzyme binding induces the formation of the closed conformation of the protein (Eklund et al., 1981), but it was also shown that crystals of LADH−NADH can be grown which are most likely in the open conformation (Cedergren-Zeppezauer, 1986). In PAC spectroscopic studies it was observed that an equilibrium of two active site geometries exists from which only one is conserved upon formation of the ternary complex LADH−NADH−DMSO (Hemmingsen et al., 1995) known to be in the closed conformation (Al-Karadaghi et al., 1994) (Figure 10). As a hypothesis it can be suggested that the LADH−NADH complex exists in an approximately 1:1 mixture of the open and the closed form of the protein independent of pH. The assumption in this work is that the isomerization step in Scheme 1 (k_2) is related to the docking of the nicotinamide ring of NAD(H). This need not necessarily involve the closure of the protein conformation.

Tryptophan luminescence studies with LADH and its complexes with coenzymes, coenzyme analogues, and ternary complexes resulted in the view that the crystallographic open and closed conformations "...are at best two gross macrostates of the protein..." (Strambini & Gonnelli, 1990). The authors found that ADPR might induce the formation of a transient conformation of the protein in the pathway of coenzyme binding and release. Room temperature phosphorescence studies showed that the binding of, e.g., one NADH or ADPR molecule to the dimer produces already all relevant structural changes in both subunits (Strambini et al., 1990). The slow isomerization process observed in this work for NADH binding (k_{-3} in Table 1) is directly related to these observations. The hypothetical mechanism presented in Scheme 2 is based on the assumption that open and closed states can exist for all ligation states of LADH. The lifetime of individual states can be strongly affected by the nature of ligands bound to the protein. In this mechanism the slow isomerisation (k_{-3}) reflects the stabilization of a "closed" conformation of both subunits after binding of one NADH molecule per dimer. In this state no additional NADH molecule can bind. The slow isomerization is observed with NADH concentrations which are several orders of magnitude higher as compared to concentrations needed to obtain complete saturation at equilibrium. Thus, the kinetically observable subunit communication has no observable effect on the thermodynamics of the complex formation. Equilibrium binding experiments (K_B in Table 1) give no indication for cooperativity of NADH binding. Furthermore, binding constants calculated from the rate constants of the simplified Scheme 1 are in excellent agreement with the data obtained in the equilibrium experiments (Table 1).

The strongest support for the above hypothesis comes from investigations of the NADH binding kinetics with the heterodimeric ES isozyme. Due to the faster binding to the S subunit a partially ordered association takes place. The first NADH molecule binds with high probability to the S subunit and stabilizes the closed conformational in both subunits which cannot bind an additional NADH molecule. Whereas the S subunit in ES-LADH shows a kinetic behavior very similar to that of SS-LADH, the limiting rate constant of 80 s^{-1} obtained for the E subunit is more than 1 order of magnitude smaller as compared to data for EE-LADH. The magnitude of the limiting rate constant for NADH association to the E subunit in ES-LADH is very similar to the data obtained for the slow isomerization observed for EE- and SS-LADH.

The question why, for example, Strambini and co-workers only detected one state of the protein at a time may be answered from the different time scales of processes observed. The rate constants for the conformational change are about 60 s^{-1} and thus by 2 orders of magnitude faster as compared to the relaxations of tryptophan phosphorescence. Thus only one average state can be observed, and the results are not in contradiction to our hypothetical mechanism.

According to Scheme 2 the transitions between open and closed conformation can also occur in the complex with both subunits loaded with NADH (K_2). We assume that the rate constant for this process is comparable to k_{-3}. From PAC spectroscopy a 1:1 equilibrium mixture of two active site geometries independent of pH was obtained. In contrast to the phosphorescence data discussed above the intermediate energy state in ^{111m}Cd-PAC spectroscopic experiments has a lifetime of 10−1000 ns and is thus so fast that two intermediates interconverting with a rate constant of 60 s^{-1} are no longer detected as an average state but as two distinct states.

Different from the LADH−NADH complex the isomerization of the LADH−NAD^+ complex is pH-dependent. At pH 7 the dissociation of the nicotinamide ring is very fast and thus responsible for the weak binding of NAD^+ as compared to NADH. Additional binding of a negatively charged ligand to the catalytic metal ion strongly stabilizes the binding of NAD^+. This effect could be part of the driving force for the deprotonation of alcohol substrates to alcoxide ions which is widely accepted as part of the catalytic mechanism. At high pH the metal ion bound water molecule is deprotonated and serves as a stabilizing factor resulting in comparable binding strength of NAD^+ and NADH at pH 10. PAC spectroscopic studies of LADH−NAD^+ complexes at various pH values resulted in data that could only be explained with a ligand geometry of the catalytic metal ion different from all X-ray structures of LADH published until

now. A reduction of the Cys-174−Cd−Cys-46 angle by approximately 20° was necessary to fit the experimental data. The same change of the metal ion geometry was found for the high-pH form of the free enzyme with OH^- bound to the cadmium ion (Hemmingsen et al., 1995). This local conformational change upon binding of NAD^+ and/or negatively charged ligands to the metal ion could be rate limiting for k_2. Thus the increase of k_2 with increasing pH could be explained from an increase of the fraction of molecules with OH^- bound to zinc where the local conformational change has already occurred. It is very likely that the local conformational change is part of the activation mechanism of LADH. Some parallels can be seen to the role of a Cys ligand in cytidine deaminase as a "valence buffer" regulating the Lewis acidity of the catalytic zinc through changes of the sulfur−zinc distance (Xiang et al., 1996).

ACKNOWLEDGMENT

We thank Zbigniew Dauter for help in making Figure 7.

REFERENCES

Adolph, H. W., Maurer, P., Schneider-Bernlöhr, H., Sartorius, C., & Zeppezauer, M. (1991) *Eur. J. Biochem. 201*, 615−625.
Al-Karadaghi, S., Cedergren-Zeppezauer, E., Hövmoller, S., Petratos, K., Terry, H., & Wilson, K. S. (1994) *Acta Crystallogr. D50*, 793−807.
Andersson, P., Kvassman, J., Lindström, A., Oldén, B., & Pettersson, G. (1981) *Eur. J. Biochem. 113*, 425−433.
Bernstein, F. C., Koetzle, T. F., Williams, G. J. B., Meyer, E. F., Jr., Brice, M. D., Rodgers, J. R., Kennard, O., Shimanouchi, T., & Tasumi, M. (1977) *J. Mol. Biol. 112*, 535−542.
Cedergren-Zeppezauer, E. S. (1986) in *Zinc Enzymes* (Bertini, I., Luchinat, C., Maret, W., & Zeppezauer, M., Eds.) pp 393−415, Birkhäuser, Boston.
Cedergren-Zeppezauer, E., Andersson, I., Ottonello, S., & Bignetti, E. (1985) *Biochemistry 24*, 4000−4010.
Coates, J. H., Hardman, M. J., Shore, J. D., & Gutfreund, H. (1977) *FEBS Lett. 84*, 25−28.
Cook, P. F., & Cleland, W. W. (1981) *Biochemistry 20*, 1805−1816.
Eftink, M. R., & Byström, K. (1986) *Biochemistry 25*, 6624−6630.
Einarsson, R., Widell, L., & Zeppezauer, M. (1976) *Anal. Lett. 9*, 815−823.
Eklund, H., & Brändén, C.-I. (1987) in *Biological Molecules and Assemblies* (Jurnak, F. A., & McPherson, A., Eds.) Vol. 3, pp 73−142, John Wiley, New York.
Eklund, H., Nordström, B., Zeppezauer, E., Söderlund, G., Ohlsson, I., Boiwe, T., Söderberg, B.-O., Tapia, O., Brändén, C.-I., & Åkeson, A. (1976) *J. Mol. Biol. 102*, 27−59.
Eklund, H., Samama, J.-P., Wallén, L., Brändén, C. I., Åkeson, Å., & Jones, T. A. (1981) *J. Mol. Biol. 146*, 561−587.
Fersht, A. (1977) *Enzyme Structure and Mechanism*, p 120, W. H. Freeman, San Francisco.
Geraci, G., & Gibson, Q. H. (1967) *J. Biol. Chem. 242*, 4275−4278.
Hemmingsen, L., Bauer, R., Bjerrum, M. J., Zeppezauer, M., Adolph, H. W., Formicka, G., & Cedergren-Zeppezauer, E. (1995) *Biochemistry 34*, 7145−7153.
Hiromi, K. (1979) *Kinetics of Fast Enzyme Reactions*, Wiley, New York.
Hol, W. G. J., van Duijnen, P. T., & Berendsen, H. J. C. (1978) *Nature 273*, 443−446.
Hubatsch, I., Zeppezauer, M., Waidelich, D., & Bayer, E. (1992) in *Advances in Experimental Medicine and Biology, Vol. 328, Enzymology and Molecular Biology of Carbonyl Metabolism 4* (Weiner, H., Crabb, D. W., & Flynn, T. G., Eds.) pp 451−455, Plenum, New York.
Hubatsch, I., Maurer, P., Engel, D., & Adolph, H. W. (1995) *J. Chromatogr. A 711*, 105−112.
Jörnvall, H., Persson, B., & Jeffrey, J. (1987) *Eur. J. Biochem. 167*, 195−201.
Kovár, J., & Klukanová, H. (1984) *Biochim. Biophys. Acta 788*, 98−109.
Kraulis, P. J. (1991) *J. Appl. Crystallogr. 24*, 946−950.
Kvassman, J., & Pettersson, G. (1979) *Eur. J. Biochem. 100*, 115−123.
Kvassman, J., & Pettersson, G. (1987) *Eur. J. Biochem. 166*, 167−172.
Li, H., Hallows, W. H., Punzi, J. S., Pankiewicz, K. W., Watanabe, K. A., & Goldstein, B. M. (1994) *Biochemistry 33*, 11734−11744.
Lively, C. R., Feinberg, B. A., & McFarland, J. T. (1987) *Biochemistry 26*, 5719−5725.
Luisi, P. L., & Favilla, R. (1970) *Eur. J. Biochem. 17*, 91−94.
Mohanty, U., Ninham, B. W., & Oppenheim, I. (1996) *Proc. Natl. Acad. Sci. U.S.A. 93*, 4342−4344.
Nicholls, A., Sharp, K., & Honig, B. (1991) *Proteins: Struct., Funct., Genet. 11*, 281−296.
Northurp, S. H., & Erickson, H. P. (1992) *Proc. Natl. Acad. Sci. U.S.A. 89*, 3338−3342.
Ohno, A., & Ushio, K. (1985) in *Coenzymes and Cofactors, Vol. II: Pyridine Nucleotide Coenzymes, Part B* (Dolphin, D., Poulson, R., & Avaraovic, Eds.) pp 105−172, Wiley, New York.
Oldén, B., & Pettersson, G. (1982) *Eur. J. Biochem. 125*, 311−315.
Park, D.-H., & Plapp, B. V. (1991) *J. Biol. Chem. 266*, 13296−13302.
Park, D.-H., & Plapp, B. V. (1992) *J. Biol. Chem. 267*, 5527−5533.
Pettersson, G. (1987) *CRC Crit. Rev. Biochem. 21* (4), 349−389.
Pietruszko, R., Ringold, H. J., Li, T.-K., Vallee, B. L., Åkeson, Å., & Theorell, H. (1969) *Nature 221*, 440−443.
Ramaswamy, S., Eklund, H., & Plapp, B. V. (1994) *Biochemistry 33*, 5230−5237.
Sayle, R. (1994) *RasMol Version 2.5. A Molecular Visualisation Program*, http://monera.ncl.ac.uk/rasmol.
Sekhar, V. C., & Plapp, B. V. (1988) *Biochemistry 27*, 5082−5088.
Stone, C. L., Bosron, W. F., & Dunn, M. F. (1993) *J. Biol. Chem. 268*, 892−899.
Strambini, G. B., & Gonnelli, M. (1990) *Biochemistry 29*, 196−203.
Strambini, G. B., Gonnelli, M., & Galley, W. C. (1990) *Biochemistry 29*, 203−208.
Taniguchi, S., Theorell, H., & Åkeson, Å. (1967) *Acta Chem. Scand. 21*, 1903−1920.
Teng, T. Y. (1990) *J. Appl. Crystallogr. 23*, 387−391.
Theorell, H., & McKinley-McKee, J. S. (1961) *Acta Chem. Scand. 15*, 1811−1833.
Theorell, H., Åkeson, Å., Liszka-Kopec, B., & De Zalenski, C. (1970) *Arch. Biochem. Biophys. 139*, 241−247.
Xiang, S., Short, S. A., Wolfenden, R., & Carter, C. W., Jr. (1996) *Biochemistry 35*, 1335−1341.
Zeppezauer, M. (1986) in *Zinc Enzymes* (Bertini, I., Luchinat, C., Maret, W., & Zeppezauer, M., Eds.) pp 417−434, Birkhäuser, Boston.

BI970398K